Available online at www.sciencedirect.com
ScienceDirect
Journal of Power Sources 176 (2008) 484–489
JOURNAL OF POWER SOURCES
www.elsevier.com/locate/jpowsour

Short communication

Decomposition of Pt–Ru anode catalysts in direct methanol fuel cells

Gyeong-Su Park [a,*], Chanho Pak [b], Young-Su Chung [a], Ji-Rae Kim [b], Woo Sung Jeon [a], Yoon-Hoi Lee [b], Kihong Kim [a], Hyuk Chang [b], Doyoung Seung [a,b]

[a] *Analytical Engineering Center, Samsung Advanced Institute of Technology, P.O. Box 111, Suwon 440-600, Republic of Korea*
[b] *Energy and Materials Research Lab, Samsung Advanced Institute of Technology, P.O. Box 111, Suwon 440-600, Republic of Korea*

Available online 2 September 2007

Abstract

The durability behavior of Pt–Ru anode catalysts under virtual direct methanol fuel cell (DMFC) operating conditions was investigated in the atomic scale using both high-resolution transmission electron microscopy (HR-TEM) and time-of-flight secondary ion mass spectroscopy (TOF-SIMS). We find here the crossover of ruthenium and platinum from the anode to the cathode due to the decomposition of active Pt–Ru anode catalysts. The Ru crossover measured at the cathode increases linearly with performance drop. The Ru contents determined by X-ray photoelectron spectroscopy (XPS) are less than 0.3 atom%. The platinum, newly deposited at the cathode with high performance drop, is formed with the intermixture of defective nanocrystalline (∼3 nm) and amorphous structure.

Keywords: Direct methanol fuel cell; Pt–Ru anode catalysts; Ru and Pt crossover; Membrane electrode assembly; Performance drop

1. Introduction

Direct methanol fuel cells (DMFCs) have been attracted great attention as promising power sources for portable electronics, which demand high power and long operation times, because of DMFC's positive characteristics such as high energy density, convenient quick recharge of fuel and ambient operating conditions [1–3]. Recently, several prototypes of DMFC system for mobile electronic devices have been announced, although technical barriers for commercialization are still existed. Among the technical issues, long-term durability of the membrane electrode assembly (MEA) is one of the most important issues [4]. Numerous studies have demonstrated that Pt–Ru alloys are the most practical anode catalysts for DMFC application due to the improvement of electro-oxidation activities [5,6]. The catalytic activity of the Pt–Ru catalyst is strongly dependent on the composition, structure, morphology, particle size and alloyed degree [7]. In the literature a number of problems related to the degradation of DMFC performance have been addressed, including (i) formation of an oxide layer on the Pt catalyst [4], (ii) Ru crossover from the anode to the cathode [8], (iii) increase of the particle size of Pt at the cathode [9,10] and (iv) degradation of the membrane and the membrane/electrode interface [11].

Regarding the polymer electrolyte membrane fuel cells (PEMFCs) system, the key factors for performance degradation, investigated using the potential cycling method [12,13], the thermal treatment method [14], and the fuel starvation method [15] are suggested as similar to the DMFC system except for the Ru crossover problems. Among those factors that deteriorate the performance, the instability of electro-catalysts under real operating conditions or accelerated conditions for rapid degradation was the most important issue that needs to be resolved quickly.

It has commonly been considered that the ruthenium deposited at the cathode by the crossover inhibits oxygen reduction kinetics and the catalytic activity. A significant motivation for the current research is the need to make clear the behavior of Pt–Ru alloy catalysts at the atomic scale, which further reveals how the Ru and Pt crossover occurs in MEA with the performance drop.

2. Experimental methods

2.1. Fuel cell preparation and durability test

The MEA for the DMFC single cell test was made by Nafion® 115 (DuPont) with the cathode and anode. The cathode was

* Corresponding author.
E-mail address: gs8144.park@samsung.com (G.-S. Park).

0378-7753/$ – see front matter © 2007 Elsevier B.V. All rights reserved.
doi:10.1016/j.jpowsour.2007.08.068

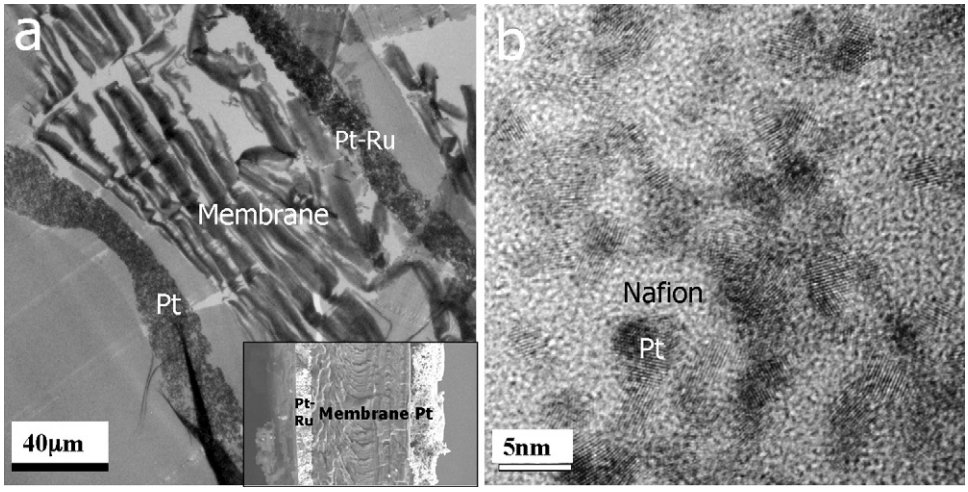

Fig. 1. (a) Typical cross-section TEM image of the MEA, which shows the layered structures of Pt–Ru anode catalysts, a membrane, and Pt cathode catalysts. The inset shows a cross-section SEM image of the same MEA. (b) High-resolution TEM image of Pt–Ru particles combined with the amorphous Nafion® binder in the DMFC anode position.

prepared by spraying Pt black (HiSpec 1000, Johnson Matthey) catalysts on carbon paper, which has a carbon microporous layer mixed with polytetrafluroethylene (PTFE). The anode was prepared by coating a slurry of Pt–Ru black (HiSpec 6000, Johnson Matthey) catalysts on a substrate film, and decaled onto the Nafion® 115 membrane. To accomplish the MEA with a 10 cm^2 active area, the catalyzed electrodes for the anode and cathode were aligned and hot-pressed at 135 °C and 5 metric tonnes for 3 min. The MEA was then assembled into a single cell fixture (consisting of graphite plates) having serpentine flow channels and gold-coated copper end plates.

During the MEA durability tests, a methanol solution (1 M, 0.3 ml A^{-1}) was delivered to the anode by a peristaltic pump at room temperature, while dry air was fed to the cathode by a mass flow controller at a 55 ml A^{-1} rate. The temperature of a single cell was controlled to maintain at 50 °C. After the test, the MEA sample was carefully taken out from the cell, labeled and frozen in liquid nitrogen for 10 min. The frozen MEA sample was immediately cut into several pieces for use in further investigations.

2.2. Characterization

Cross-sections of the MEAs for scanning electron microscopy (SEM) observation were prepared by breaking the samples after dipping them in liquid nitrogen. Thin cross-sections of the MEAs for transmission electron microscopy (TEM) observation were prepared by ultramicrotomy after embedding them in epoxy resin. The thickness of the sample was about 60–70 nm. The SEM and TEM observations were performed using a HITACHI S-4700 at an accelerating voltage of 15 kV and a TECNAI F-30 at an accelerating voltage of 300 kV, respectively. The TEM is capable of nano-EDS (energy-dispersive X-ray spectroscopy) analyses in scanning transmission electron microscopy (STEM) mode by positioning a small probe in the Z-contrast STEM images. Time-of-flight

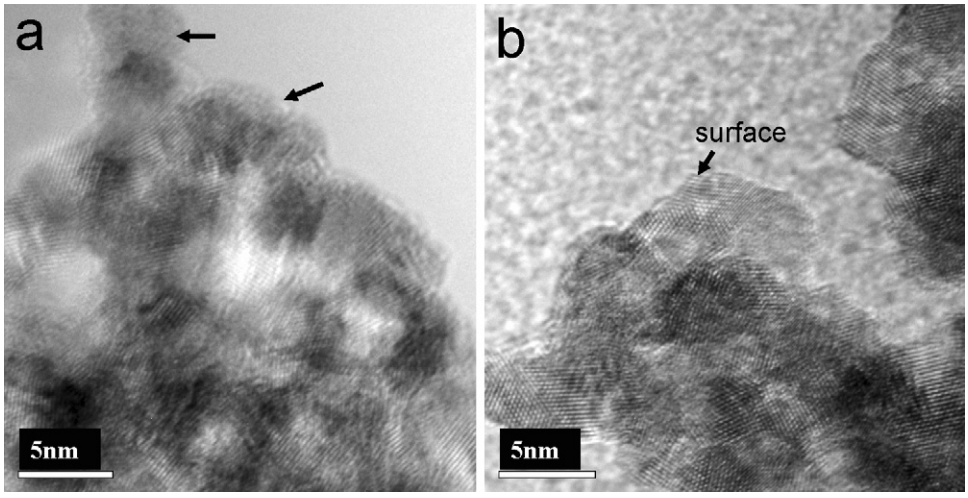

Fig. 2. High-resolution TEM images observed at pristine Pt–Ru particles (a) and at Pt–Ru particles (b) after hot-pressing. The pristine Pt–Ru particles are covered with thin amorphous films as indicated by arrows. A clean surface of the Pt–Ru agglomeration is obtained after the hot-pressing.

secondary ion mass spectroscopy (TOF-SIMS) measurements were performed using an ION-TOF IV. Ru ion images were obtained using 25 keV Bi^{1+} primary ions over 500 μm × 500 μm with 256 × 256 pixels.

3. Results and discussion

Fig. 1a shows a typical cross-section TEM image of the MEA, which clearly demonstrates the layered structures of Pt–Ru anode catalysts, a membrane, and Pt cathode catalysts. The inset shows a cross-section SEM image observed in the same MEA sample. Although there is a small difference in the roughness of the Pt–Ru anode layer between the TEM image and the SEM image, we carefully measured the thickness of the Pt layer, the membrane, and the Pt–Ru layer as about 10–30 μm, 90 μm, and 15 μm, respectively. A high-resolution TEM (HR-TEM) image of the Pt–Ru particles is shown in Fig. 1b. The HR-TEM image supports that spherical Pt–Ru particles, 2.7–3.5 nm in size, are well combined with the amorphous Nafion® binder in the DMFC anode position.

Comparison of Fig. 2a and b indicates that pristine Pt–Ru particles (FC-1) are covered with thin (less than 1 nm) amorphous films at the surface, but the amorphous films are removed after hot-pressing as shown in Fig. 2b. Note that a clean surface of the Pt–Ru agglomeration is obtained after the hot-pressing. Atomic structure changes of Pt–Ru particles after performance degradation are another notable observation for understanding the detailed decomposition process of Pt–Ru particles. Fig. 3a shows an HR-TEM image of the Pt–Ru particle observed after a test for 182 h (FC-2). The durability test was performed intermittently under the potentio-static mode at 0.4 V for 2 h on each day. The resulting performance drop was 34%. The Pt–Ru particle has partly transformed from an initial spherical shape to a conical shape. Line profiles (Fig. 3b), precisely measured at L1 and L2 positions of Fig. 3a, unambiguously exhibit the atomic distance change in the Pt–Ru particle. The atomic distance measured at L1 corresponds to the {1 2 0} plane of Pt–Ru alloy indicated by a dotted line in Fig. 3a. Further confirmation of the atomic distance change is clearly displayed from the digital diffractogram of Fig. 3c, which shows an additional A2 spot nearby the fundamental A1 spot. The A1 spot corresponds to the reflection of the (1 2 0) plane of the Pt–Ru particle. Fig. 4a shows another HR-TEM image of the Pt–Ru particle (~3.5 nm) observed after the 182 h durability test (FC-2), which demonstrates the crack occurring across the particle surface, indicated by the arrows. A line profile (Fig. 4b) measured around the crack position indicated by a dotted line in Fig. 4a strongly suggests an increase (0.7 Å) in atomic distance caused by the crack spread. Fig. 4c shows an HR-TEM image of Pt–Ru particles observed after a 128 h durability test (FC-3). Intermittently, low voltage (0.35 V) and long operation time (8 h on each day) were applied to rapidly degrade the performance. The resulting performance drop was 45%. The image clearly supports that the Pt–Ru particles (indicated by red circles) at the anode are decomposed into small particles through the morphological change (Fig. 3a) and the cracking (Fig. 4a) during the performance degradation. The particle size was estimated to be about 1.2–2.5 nm. This result suggests that the small particles may be readily oxidized into ionic Pt and Ru species, and move across the membrane under virtual DMFC operating conditions.

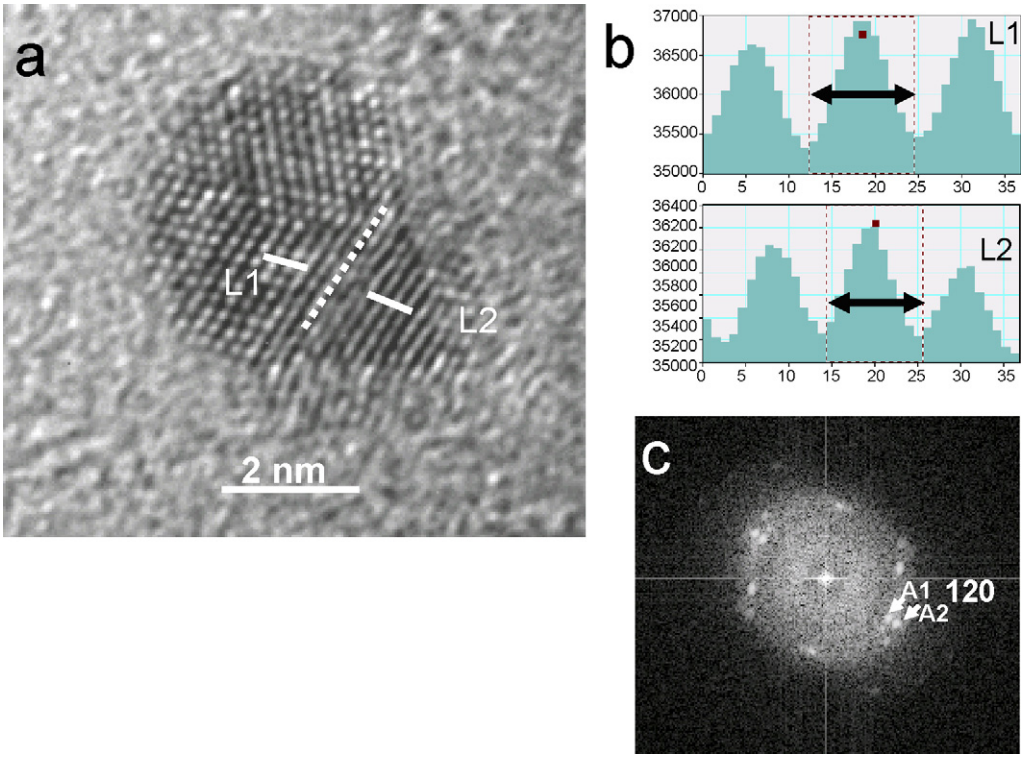

Fig. 3. (a) High-resolution TEM image of the Pt–Ru particle observed after a test for 182 h (FC-2). Cell voltage: 0.35 V; temperature: 50 °C; anode: 1.0 M methanol. (b) Line profiles measured at L1 and L2 positions of (a). (c) Digital diffractogram of (a).

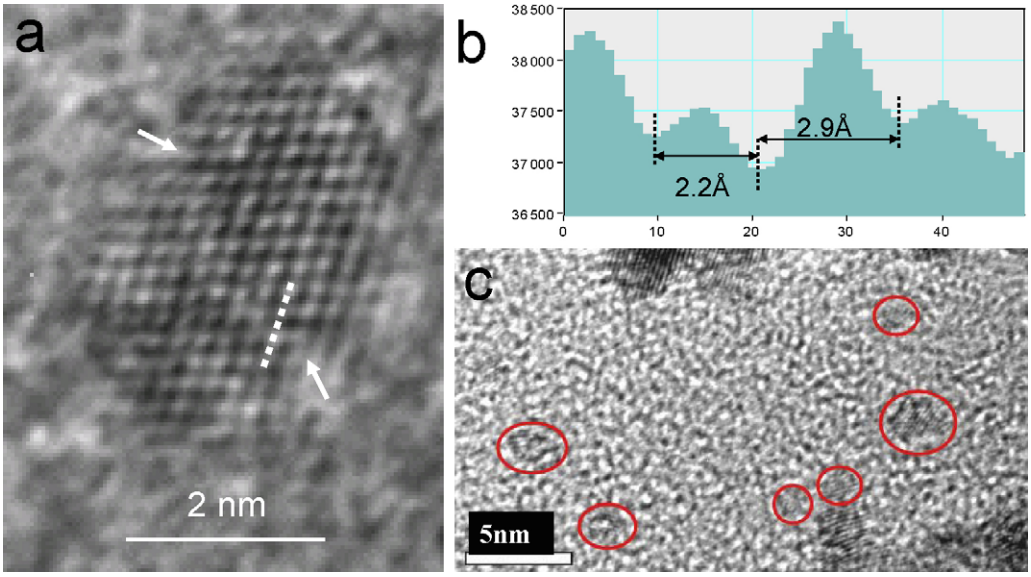

Fig. 4. (a) Another high-resolution TEM image of a Pt–Ru particle observed after the 182 h durability test. (b) Line profile measured around the crack position indicated by a dotted line in (a). (c) HR-TEM image of Pt–Ru particles observed after a test for 128 h (FC-3). Low voltage (0.35 V) and long operation time (8 h on each day) were applied. Red circles indicate the Pt–Ru particles decomposed into small particles. (For interpretation of the references to color in this figure legend, the reader is referred to the web version of the article.)

To confirm that the decomposed Pt–Ru particles travel across a membrane from the anode to the cathode, we closely investigated the cross-section of a membrane to find the deposited particles in the membrane due to the reduction of ionic Pt and Ru species. The MEA sample studied was obtained after an accelerated test. For the accelerated test, high potential up to 1.4 V was applied to the anode by a pulse method. A high-angle annular dark-field (HAADF) image observed at the cross-section region of the membrane, shown in Fig. 5a, clearly illustrates that small particles are partly deposited in the membrane layer. The EDS result, indicated in Fig. 5b, verifies that the deposited particles in the membrane are platinum. The fluorine peak in the EDS spectrum originates from a Nafion® membrane.

Three cathodes in the tested cells were sampled for TOF-SIMS analyses. Those samples were varied in their performance drop, as (A) 17%, (B) 21% and (C) 45%. Fig. 6 shows SIMS mapping images of the Ru^+ ion obtained at the as-pressed cathode and the three tested cathodes, respectively. Although all EDS results for the tested cathodes did not reveal the presence of any Ru peak, the SIMS mapping images clearly illustrate that the Ru accumulation at the cathode surface increases linearly with the performance drop. Quantitative X-ray photoelectron spectroscopy (XPS) results yield evidence that the Ru contents in the three cathodes are less than 0.3 atom%.

The SIMS mapping images shown in Fig. 6 unambiguously provide evidence of ruthenium crossover through the decomposition of Pt–Ru catalysts, whereas the Pt crossover to the cathode is not clear despite the discovery of Pt particles in the membrane (Fig. 5) because the Pt particles also can be moved from the cathode [12]. Pt-to-Ru atomic ratios were determined by EDS for the three Pt–Ru anode catalysts labeled FC-1, FC-2, and FC-3 in order to examine how the crossover of Pt and Ru influences

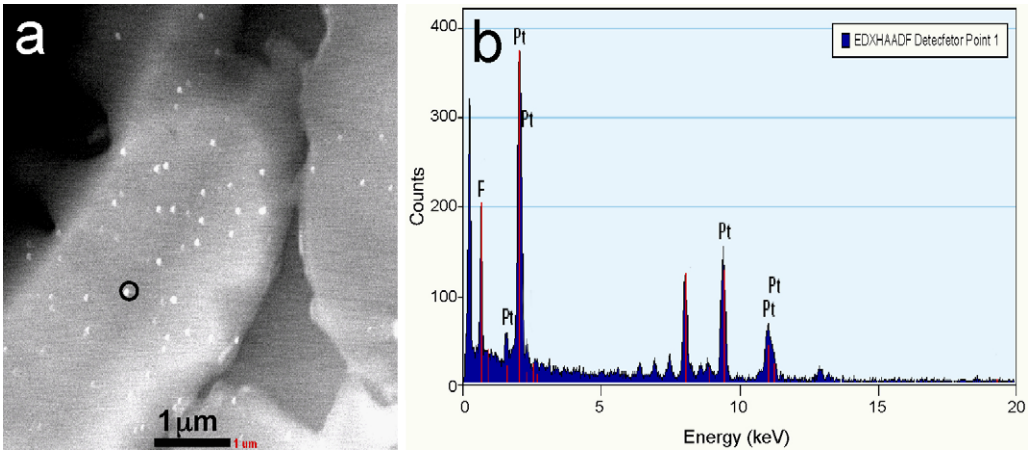

Fig. 5. (a) HAADF image observed at the cross-section region of Nafion® membrane. The sample was obtained after an accelerated test. Small particles are partly deposited in the membrane. (b) EDS result obtained from a particle indicated by a solid circle in (a).

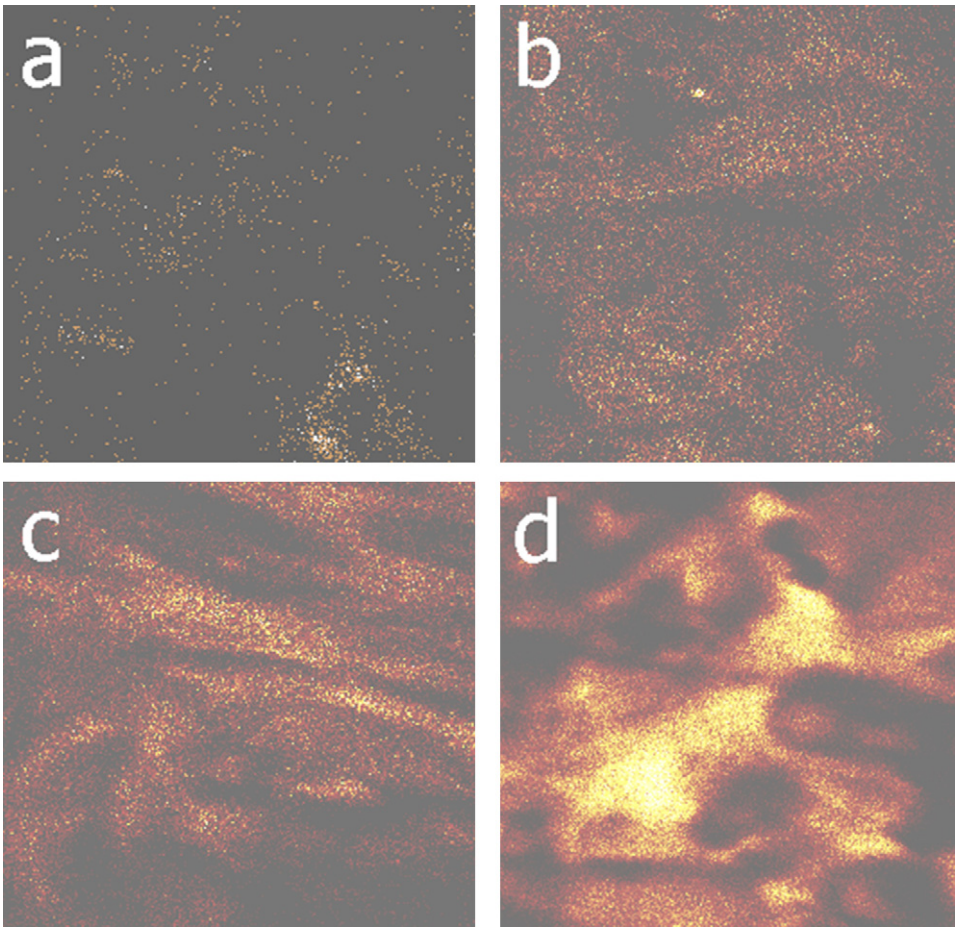

Fig. 6. TOF-SIMS mapping images of the Ru^+ ion obtained at the as-pressed cathode (a) and the three tested cathodes, respectively. The three tested cathodes were varied in their performance drop, as 17% (b), 21% (c), and 45% (d). The mapping area was 500 μm × 500 μm.

the compositional changes at the anodes; these data are summarized in Table 1. If the Ru crossover occurred alone during the performance drop, the fraction of Pt in the Pt–Ru particles should be increased. However, note the gradual decrease of the Pt fraction as the performance drop increases. This strongly supports that the Pt crossover from the anodes takes place with the performance drop. Recent studies have shown how platinum tends to preferentially dissolve under PEMFC operating conditions [16,17]. Similarly, our results indicate that the Pt crossover from anode associates with the morphological change of Pt–Ru particles and the formation of soluble platinum species in the particle surfaces. The Ru enrichment induced at the anodes can

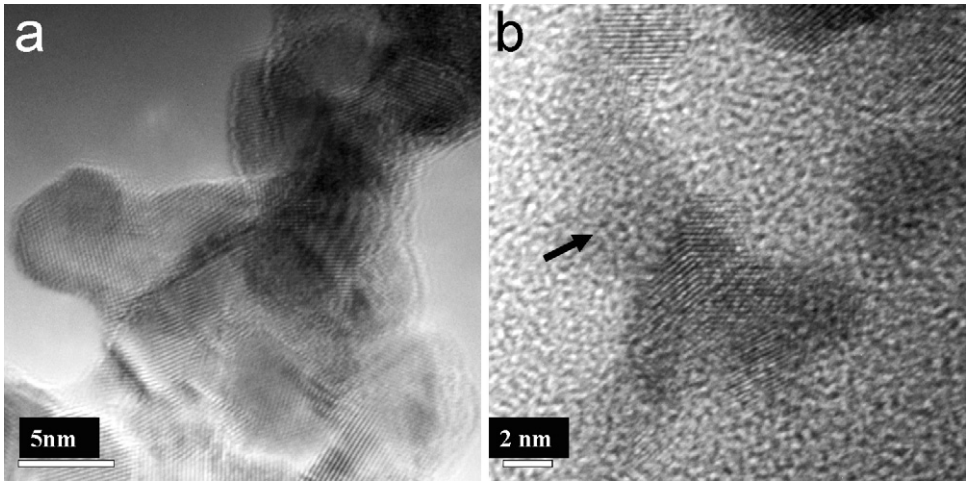

Fig. 7. High-resolution TEM images observed at the pristine Pt cathode particles (a) and at the highly degraded Pt cathode particles (b) after a 128 h durability test. Newly formed amorphous phase is indicated by an arrow in (b).

Table 1
Pt-to-Ru atomic ratios determined by EDS for the three Pt–Ru anode catalysts labeled FC-1, FC-2 and FC-3

Samples	Pt	Ru
FC-1 (pristine Pt–Ru)	63.0 ± 2.0	39.0 ± 2.0
FC-2 (34% performance drop)	53.0 ± 2.5	47.0 ± 2.5
FC-3 (45% performance drop)	44.8 ± 0.9	55.2 ± 0.9

decrease the methanol oxidation activity. The modification of Pt cathode surface by the Ru contamination also results in a decay of the oxygen reduction activity.

As the cathode consists of platinum catalysts, it is really difficult to find any traces of the Pt crossover at the cathode. Fig. 7a and b show HR-TEM images observed at the pristine Pt cathode particles (a) and at the highly degraded Pt cathode particles (b) after a 128 h durability test. The comparison of the HR-TEM images shows that defective nanocrystals (∼3 nm) and an amorphous phase (dark contrast area indicated by an arrow in Fig. 7b) are newly formed in the initial Pt cathode particles (∼6 nm) after a test for 128 h. The fact that nano-EDS results show only Pt peak at their position suggests that they may come from Pt–Ru anode catalysts by the Pt crossover. Consequently, the main point is that ruthenium and platinum may decompose from the highly active Pt–Ru anode catalysts, move across the Nafion® electrolyte membrane, and redeposit at the Pt cathode on the opposite side of the MEA under normal DMFC operating conditions.

4. Conclusions

In DMFC operation, we found that ruthenium and platinum in Pt–Ru anode move through the Nafion® electrolyte membrane to the Pt black cathode during the durability tests. The microstructures observed by HR-TEM coupled with nano-EDS analyses strongly suggest that the Pt–Ru anode catalysts decompose into small particles through their morphological change and cracking. The Pt and Ru ions formed by the decomposition process move across the solid electrolyte membrane and redeposit at the Pt cathode. TOF-SIMS mapping images at the cathode surface support that the Ru crossover rate linearly increases as the cell performance drop. Quantitative XPS results yield evidence that the Ru contents accumulated at the cathode are less than 0.3 atom%. Moreover, Pt crossover was confirmed by the compositional changes of Pt–Ru anode catalysts as well as the Pt particles deposited in the membrane layer. The platinum, newly deposited at the cathode with high performance drop, is formed with the intermixture of defective nanocrystalline (∼3 nm) and amorphous structure.

References

[1] H. Chang, I. Song, D. Seung, Small Fuel Cells for Portable Applications, in: Proceedings of the 8th Small Fuel Cells 2006, Washington DC, USA, April 3–4, 2006.
[2] A.S. Arico, S. Srinivasan, V. Anonucci, Fuel Cells 1 (2001) 133–161.
[3] F. De Brujin, Green Chem. 7 (2005) 132–150.
[4] C. Eickes, P. Piela, J. Davey, P. Zelenay, J. Electrochem. Soc. 153 (2006) A171–A178.
[5] F. Maillard, G.-Q. Lu, A. Wieckowski, U. Stimming, J. Phys. Chem. B 109 (2005) 16230–16243.
[6] H. Liu, C. Song, L. Zhang, J. Zhang, H. Wang, D.P. Wilkinson, J. Power Sources 155 (2006) 95–110.
[7] H.N. Dinh, X. Ren, F.H. Garzon, P. Zelenay, S. Gottesfeld, J. Electroanal. Chem. 491 (2000) 222–233.
[8] P. Peila, C. Eickes, E. Brosha, F. Garzon, P. Zelenay, J. Electrochem. Soc. 151 (2004) A2053–A2059.
[9] H. Kim, S.-J. Shin, Y.-G. Park, J. Song, H.-T. Kim, J. Power Sources 160 (2006) 440–445.
[10] M.K. Jeon, K.R. Lee, K.S. Oh, D.S. Hong, J.Y. Won, S. Li, S.I. Woo, J. Power Sources 158 (2006) 1344–1347.
[11] T. Kinumoto, M. Inaba, Y. Nakayama, K. Ogata, R. Umebayashi, A. Tasaka, Y. Iriyama, T. Abe, Z. Ogumi, J. Power Sources 158 (2006) 1222–1228.
[12] K. Yasuda, A. Taniguchi, T. Akita, T. Ioroi, Z. Siroma, Phys. Chem. Chem. Phys. 8 (2006) 746–752.
[13] R.L. Borup, J.R. Davey, F.H. Garzon, D.L. Wood, M.A. Inbody, J. Power Sources 163 (2006) 76–81.
[14] M. Cai, M.S. Ruthkosky, B. Merzougui, S. Swathirajan, M.P. Balogh, S.H. Oh, J. Power Sources 160 (2006) 977–986.
[15] A. Taniguchi, T. Akita, K. Yasuda, Y. Miyazaki, J. Power Sources 130 (2004) 42–49.
[16] R.M. Darling, J.P. Meyers, J. Electrochem. Soc. 150 (2003) A1523–A1527.
[17] P.J. Ferreira, G.J. Ia O', Y. Shao-Horn, D. Morgan, R. Makharia, S. Kocha, H.A. Gasteiger, J. Electrochem. Soc. 152 (2005) A2256–A2271.